DOI: 10.61782/fa.2025.0273

DESIGN AND OPTIMISATION OF A MULTI-LAYER POROUS BARRIER WITH TUNABLE RESONATORS

Laura Sousa[1*] **Luís Godinho**[1] **Paulo Amado Mendes**[1]
[1] University of Coimbra, ISISE, ARISE, Department of Civil Engineering, Coimbra, Portugal

ABSTRACT

Complementing the effect of porous materials with embedded resonators can be a simple and effective strategy to improve sound absorption of traffic noise barriers. Although several studies exist in the literature, few practical applications can be found, and there is ample room for defining optimized configurations that may allow improving, for example, their low frequency behaviour. For the specific case of embedded resonant structures, introducing multiple elements with different resonant frequencies, and allowing for different neck geometries may be a possible way of obtaining such improvement.

Here, the development of a carefully designed acoustic barrier is addressed. A metasurface is introduced, consisting of a porous multi-layer system into which tuned resonators are integrated. Both the multi-layer arrangement and the resonators optimise targeting specific frequency ranges. For the case of the resonators, optimal designs are obtained by adjusting their dimensions, neck geometry and number of different resonators employed. Modelling is performed using the Transfer Matrix Method and validated by means of a Finite Element Method, and good agreement between the two methods has been observed. The final results demonstrate the possibility of defining practical and effective solutions for application in noise barriers in the context of traffic noise mitigation.

Keywords: *Transfer Matrix Method, Metasurface, Sound Absorption, Porous Noise Barriers.*

[*]***Corresponding author***: lrldsousa@hotmail.com.

1. INTRODUCTION

Traffic-related noise in Western Europe was estimated to result in the loss of one million healthy life years, thereby highlighting the considerable public health challenges associated with environmental noise sources such as road, railway, and air traffic, as well as construction sites, which have been linked to adverse health outcomes including cardiovascular diseases, sleep disturbances, and cognitive impairment [1]. Addressing this problem, porous and fiber materials [2], resonators [3], metamaterials [4] and barriers [5], play a key role for acoustic purposes. Thus, metaporous surfaces offer an excellent compromise between the broadband performance of porous layers and the deep subwavelength properties of metasurfaces [6]. Given that their absorption properties depend on a complex interaction between thermal and viscous losses within the porous layer and the resonant elements [7]. Therefore, finding the optimal combination of different systems is of great practical value, as it allows for attenuation across broader frequency ranges with high sound absorption.

In this work, a porous metasurface was designed to achieve high absorption over a broad frequency range. Due to the lack of sound absorption, at low frequencies, by the porous materials [8], by integrating slit-shaped resonant inclusions within the solid matrix, the low-frequency performance is notably enhanced. These resonators increase the dissipation of acoustic energy through thermal and viscous losses occurring within the pores [9].

A multilayer acoustic barrier has been considered. It consists of a porous multilayer system, characterized in this work by an equivalent fluid model [10] and the incorporation of

resonators described using formulas proposed by Stinson [11]. The complete system was assembled using the Transfer Matrix Method (TMM) [4], which was validated both by the Finite Element Method (FEM) [12] and through experimental tests in an impedance tube [13].
A parametric analysis was conducted to assess how the geometry and arrangement of the slit inclusions influence the overall absorption. Analytic and numerical results demonstrate that the suggested metamaterial attains significantly higher low-frequency absorption compared to the porous layer without the inclusions.

2. METHODOLOGY

In this work, the objective was to develop a metasurface comprising a porous multilayer system with embedded resonators (Figure 1). Initially, an extensive study was undertaken to characterise the porous material, in this case, porous concrete [14-17]. Subsequently, different slit-type resonators were examined. The Transfer Matrix Method was the chosen approach for this research.

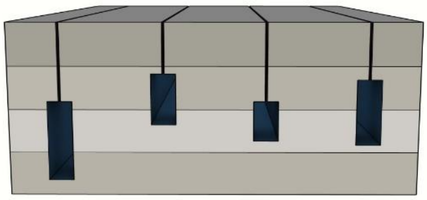

Figure 1. Porous metasurface with resonators inclusions

With regard to the porous concrete made with expanded clay (Figure 2), previous studies have been conducted to determine its acoustic properties, including macroscopic parameters, as well as a comprehensive assessment of its sound absorption and surface impedance [14-17].

(a) (b)

Figure 2. Porous concrete samples (a) and details of the porous concrete material (b)

This earlier work encompassed both experimental and numerical aspects. In the present study, certain results from that prior investigation were used, notably the pre-established relationships between the material's density and porosity and the remaining macroscopic parameters, followed by the determination of the sound absorption curve. The intention is to employ this porous material made with expanded clay in a noise barrier, prompting the idea of creating a multilayer porous system using the same base material. For this purpose, the macroscopic parameters of each layer were optimised based on the model proposed by Horoshenkov and Swift [10], thereby yielding an optimised sound absorption curve in comparison to a non-optimised multilayer system. The Transfer Matrix Method was adopted, relating the sound pressure and the normal velocity of acoustic particles at the two faces of each layer [4].
Subsequently, a study was carried out on the acoustic behaviour of slit-type resonators. The equivalent fluid model proposed by Stinson [11] was employed to characterise both the neck and the cavity. For slit geometries, the effective density and bulk modulus expressions are derived from those for rectangular cross-section tubes, under the assumption that one dimension is significantly larger than the other [4]. Once again, the Transfer Matrix Method was used to describe the overall behaviour and to obtain the sound absorption curve. In addition, the sound absorption curve was optimised for specific frequencies.

Various configurations have been studied, in which the number of porous layers as well as the number and geometry of the resonators have varied (not all configurations here presented). To validate the methodology employed, equivalent systems were simulated using the Finite Element Method (FEM), and experimental validation tests were performed with the two microphones impedance tube method [13]. In the experimental validation, melamine was used as the porous material (Figure 3), and for its theoretical simulation, the more appropriate Delaney-Bazley-Miki model (DBM) [18] was chosen.

(a) (b)

Figure 3. Melamine samples (a) and details of the melamine porous material (b)

From the experimental campaign, the sound absorption curves for melamine and for the complete system, comprising a single layer of melamine with the inclusion of one slit resonator, were obtained. Additive manufacturing was used to manufacture the previously tailored slit resonators (Figure 4).

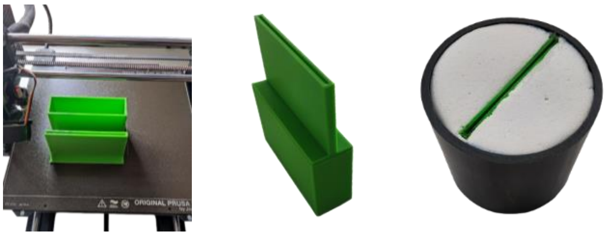

(a) (b) (c)

Figure 4. Slit resonator (a) and (b), samples for sound absorption: system made of melamine and a slit resonator embedded (c)

The samples of melamine are 102 mm thick and a diameter of 100 and 38 mm, and the samples with the full system, melamine and slit resonator, are 102 mm thick and have a diameter of 100 mm. The resonator has internal dimensions as in Figure 5:

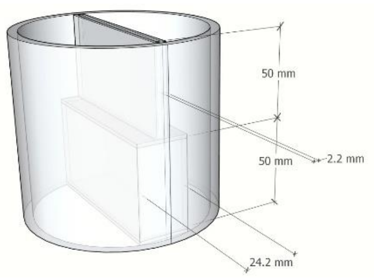

Figure 5. Schematic samples for sound absorption: system made of melamine and a slit resonator

2.1 Transfer Matrix Method (TMM)

The TMM allows estimating how sound waves are transmitted and reflected through a system of acoustic components (Figure 6), such as multilayer porous assemblies [8]. It establishes the relationship between acoustic pressure and particle velocity at the system's input and output ports, considering the acoustic characteristics of each element as well as the overall system geometry. Consequently, it serves as an excellent tool for predicting sound absorption and transmission loss of laterally infinitely layered multilayer materials arranged in series[4].

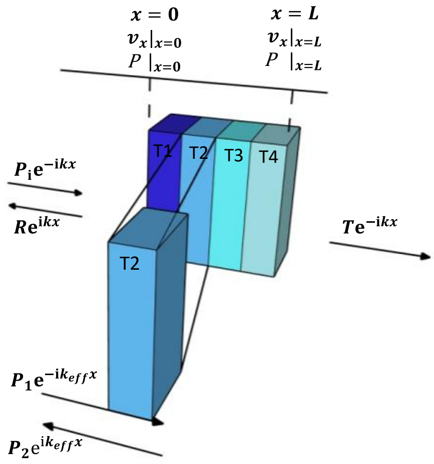

Figure 6. Scheme of an acoustic multilayer structure

The transfer matrix between the two faces of an isotropic and homogeneous 1D material, from x = 0 to x = *l*, is used to relate the sound pressure, *p*, and the normal velocity of acoustic particles, *v*, at the two faces of a single layer of material:

$$\begin{bmatrix} p \\ v \end{bmatrix}_{x=0} = \begin{bmatrix} \cos(kl) & \mathrm{i}Z\sin(kl) \\ \mathrm{i}\sin(kl)/Z & \cos(kl) \end{bmatrix} \begin{bmatrix} p \\ v \end{bmatrix}_{x=l}, \quad (1)$$

in which the wave number of the material is defined as $k = \omega/c = \omega\sqrt{\rho/K}$, with ω being the angular frequency, c the speed of sound propagation, ρ the density, and K the bulk modulus. The acoustic impedance is defined as $Z = \sqrt{\rho K}$, and $\mathrm{i} = \sqrt{-1}$ is the imaginary unit. A Fourier time convention $\mathrm{e}^{\mathrm{i}\omega t}$ is assumed. The transfer matrix, T, considering a two-layered system, with layers A and B, can be written as:

$$\mathrm{T} = \mathrm{T}_A \mathrm{T}_B \quad , \quad (2)$$

with:

$$\mathrm{T}_A = \begin{bmatrix} \cos(k_A l_A) & \mathrm{i}Z_A\sin(k_A l_A) \\ \mathrm{i}\,\sin(k_A l_A)/Z_A & \cos(k_A l_A) \end{bmatrix}, \quad (3)$$

$$\mathrm{T}_B = \begin{bmatrix} \cos(k_B l_B) & \mathrm{i}Z_B\sin(k_B l_B) \\ \mathrm{i}\,\sin(k_B l_B)/Z_B & \cos(k_B l_B) \end{bmatrix}, \quad (4)$$

Finally, the total transfer matrix, is given by the product of the transfer matrices of the N elements of the overall system.

$$\mathrm{T} = \prod_{n=1}^{N} \mathrm{T}_n \quad (5)$$

For parallel layers, the transfer matrix between the two faces of a homogeneous and isotropic 1D material, extending from x = 0 to x = *l*, that relates the sound pressure, p, and the normal velocity of acoustic particles, v, at the two faces is:

$$\begin{bmatrix} v_1 \\ v_2 \end{bmatrix} = \begin{bmatrix} Y_{11} & Y_{12} \\ Y_{21} & Y_{22} \end{bmatrix} \begin{bmatrix} p_1 \\ p_2 \end{bmatrix}, \quad (6)$$

where, p_1 and p_2, are the sound pressure, v_1 and v_2 are the normal velocity of acoustic particles, at the two faces, Y_{11} and Y_{22} are the self-admittances and Y_{12} and Y_{21} are the transfer-admittances calculated with:

$$Y_A = \begin{bmatrix} Y_{11}^A & Y_{12}^A \\ Y_{21}^A & Y_{22}^A \end{bmatrix} = \begin{bmatrix} -\mathrm{i}\frac{\cos(k_A l_A)}{Z_A \sin(k_A l_A)} & \mathrm{i}\frac{1}{Z_A \sin(k_A l_A)} \\ -\mathrm{i}\frac{1}{Z_A \sin(k_A l_A)} & \mathrm{i}\frac{\cos(k_A l_A)}{Z_A \sin(k_A l_A)} \end{bmatrix} \quad (7)$$

$$Y_B = \begin{bmatrix} Y_{11}^B & Y_{12}^B \\ Y_{21}^B & Y_{22}^B \end{bmatrix} = \begin{bmatrix} -\mathrm{i}\frac{\cos(k_B l_B)}{Z_B \sin(k_B l_B)} & \mathrm{i}\frac{1}{Z_B \sin(k_B l_B)} \\ -\mathrm{i}\frac{1}{Z_B \sin(k_B l_B)} & \mathrm{i}\frac{\cos(k_B l_B)}{Z_B \sin(k_B l_B)} \end{bmatrix} \quad (8)$$

And, in terms of admittances matrices, a parallel combination of n layers means that they all share the same pressure across two faces:

$$Y_{\text{total}} = \sum_{n=1}^{N} Y_{n\ resonator} + \sum_{m=1}^{M} Y_{m\ porous} * A_{sur}, \quad (9)$$

where each Y_n is the admittance matrix of a resonator and each Y_m is the admittance matrix of a porous layer. A_{sur} is the surface area of the porous material.

2.2 Finite Element Method (FEM)

In this study, the Finite Element Method (FEM) was employed to validate the predictions made using the TMM. The FEM analysis involved discretising the acoustic domain into finite elements and solving the governing wave equation in the frequency domain [12]. The medium's properties, its density (ρ) and speed of sound (c), are fundamental in defining the Helmholtz equation, which . In acoustics, the propagation of sound waves is typically described written as:

$$\nabla^2 P + \left(\frac{\omega^2}{c^2}\right) P = 0\,, \quad (10)$$

in which: $\omega=2\pi f$ is the angular frequency and P is the acoustic pressure. Adequate boundary conditions are employed to account for the interaction between the acoustic waves and the geometry's boundaries. The sound absorption coefficient, α, is calculated based on the pressure measured at diverse points:

$$\alpha = 1 - |R|^2 \quad (11)$$

in which R is the reflectance, that depends on the phase difference between the reflected and incident waves:

$$R = \frac{H - \mathrm{e}^{-\mathrm{i}ks}}{\mathrm{e}^{\mathrm{i}ks} - H} \quad (12)$$

where: H is the ratio of the pressures at the two selected points P_1 and P_2, k is the wave number and s is the distance between P_1 and P_2.

2.3 Impedance Tube

To characterize the sound absorption coefficient with normal incidence, tests were performed on circular impedance tubes with 100 and 38 mm in diameter (Figure 7). This standardised technique provided reliable measurements of sound absorption coefficients under normal incidence conditions [13].

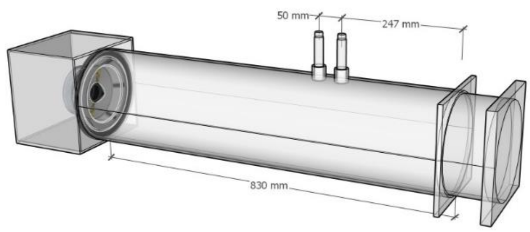

Figure 7. Scheme of 100 mm impedance tube

The test methodology is indicated in ISO 10534-2 [13], where the sound absorption coefficient, α, is calculated according to:

$$\alpha = 1 - |R|^2 \quad (13)$$

where R is the reflection coefficient as defined in Equation 12.

3. RESULTS AND ANALYSIS

3.1 Experimental model validation

In order to characterize the acoustic absorption properties of the system under study, the impedance tube method, was employed [13]. The experimental data obtained were subsequently used to validate the TMM model applied in this study. By comparing the TMM predictions with the experimental results from the impedance tube, the accuracy and applicability of the model in predicting the acoustic performance of the multilayered system were confirmed (Figure 8 and Figure 9). The experimental melamine sound absorption curve (α_{EXP_mela}) and the theoretical Delany–Bazley–Miki (α_{DBM}) curve follow similar trends, confirming that the DBM model generally captures the main absorption characteristics of melamine. Discrepancies, typically at lower frequencies, reflect the empirical nature of DBM and potential real-world factors in the experimental sample. The slit resonator (α_{TMM_slit}) exhibits a sharp absorption peak at its resonant frequency, effectively targeting lower frequencies with a narrowband. When the theoretical slit resonator is combined with melamine (modelled with DBM), the resulting curve shows enhanced absorption in the low-frequency region, due to the resonator, while still retaining the broad mid- to high-frequency absorption typical of melamine. This synergy provides a wider effective absorption bandwidth than either component alone.

Overall, the obtained results suggest that incorporating a slit resonator with a porous material can yield a more comprehensive absorption profile across the frequency spectrum, especially useful in applications demanding improved low-frequency performance (Figure 8).

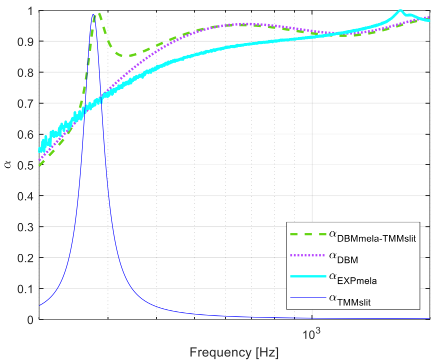

Figure 8. Sound absorption coefficient for melamine, slit and full system

In Figure 9, the theoretical prediction obtained by combining the experimental absorption data of melamine with the TMM model for the slit resonator, based on Stinson's formulation, ($\alpha_{EXPmela+TMMslit}$) and the experimental absorption measured for the physical sample comprising melamine plus the slit resonator ($\alpha_{EXP-(mela+slit)}$) are represented.

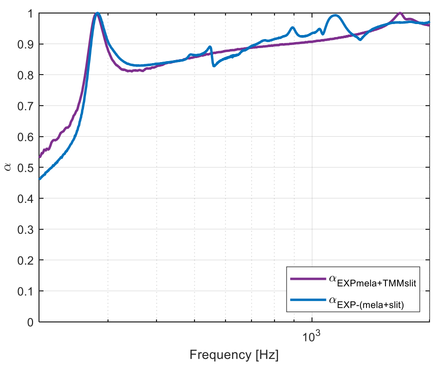

Figure 9. Sound absorption coefficient of full system. Experimental data and TMM estimated results

The good agreement between the sound absorption curve predicted by the TMM model and the experimental results suggests that the model is suitable for predicting the sound absorption coefficient of this type of system (a porous material with the inclusion of slit-type resonators). In particular, the coincidence of resonance peaks and the similar behaviour across different frequency ranges indicate that the method accurately describes the acoustic propagation, the interactions among the porous layers, and the slit resonance effects. Consequently, the application of TMM to predict the acoustic performance in this case is validated, providing confidence in its use for the analysis, optimisation, and design of multilayer systems with resonators.

3.2 Metaporous surface, analythical and numerical results

Complementarily, a verification was also carried out using the FEM methodology, now considering a layered system with porous concrete. There is a good agreement between both curves across almost the entire frequency range (Figure 10), reinforcing the validity of the TMM as an analysis tool for this type of multilayer system with embedded resonators. Some discrepancies at certain frequencies may be due to model simplifications, as well as the FEM model's ability to account for reflections within the porous medium resulting from contact with the resonator's rigid surface. Overall, the correspondence between the results demonstrates the consistency of the TMM model, suggesting that it is indeed possible to simulate such systems at a lower computational cost.

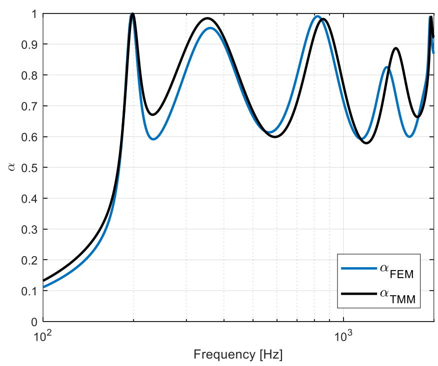

Figure 10. Metasurface with 4 porous layers and 1 embedded resonator obtained with FEM and TMM models

Figure 11 shows the performance of a metasurface system, composed of 2 porous layers and 3 resonators, using the TMM. The resonators' curves ($\alpha_{TMMres250}$, $\alpha_{TMMres285}$,

$\alpha_{TMMres300}$) represent the individual responses of each resonator, each displaying a distinct absorption peak at its respective resonance frequency. These peaks clearly indicate the resonators' effectiveness in targeting and attenuating sound within specific frequency bands. The overall system performance ($\alpha_{TMMporous+resonators}$) demonstrates a broadened absorption across the frequency spectrum. This enhanced broadband absorption results from the combination of the porous layers' inherent wideband absorption and the narrowband contributions of the resonators.

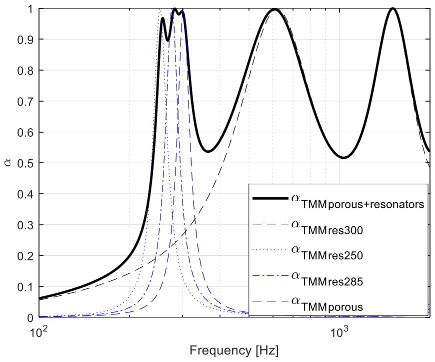

Figure 11. TMM simulation of a Metasurface with 2 porous layers and 3 embedded resonators

The good agreement between both the individual resonator curves and porous curve and the metasurface response validates the design approach, suggesting that the TMM model accurately captures the acoustic interactions within such multilayer systems. Consequently, this method appears to be a reliable and computationally efficient tool for the analysis, optimisation, and design of advanced acoustic barriers and metasurfaces.

4. FINAL REMARKS

The results obtained with the Transfer Matrix Method (TMM) support the effectiveness of integrating porous layers with slit-type resonators to achieve enhanced acoustic absorption. The distinct resonance peaks of the individual resonators, as well as the porous layers' absorption curve, correspond well with the broader absorption observed in the composite system, underscoring the synergistic benefits of this type of design. These conclusions confirm that the TMM is an accurate and computationally efficient tool for predicting the acoustic performance of multilayer systems, also allowing the inclusion of resonators.

Furthermore, the theoretical predictions for the porous material have been supported by experimental measurements, reinforcing the reliability of the baseline model. The successful combination of the narrowband effects of the resonators with the broadband absorption properties of the porous layers offers promising prospects for optimising noise reduction across a wide frequency range. This paves a way for innovative advancements in the design and optimisation of acoustic barriers and metasurfaces.

5. ACKNOWLEDGMENTS

This work is financed by national funds through FCT - Foundation for Science and Technology, under grant agreement 2023.05188.BD awarded to the 1st author, and partly financed by FCT / MCTES through national funds (PIDDAC) under the R&D Unit Institute for Sustainability and Innovation in Structural Engineering (ISISE), under reference UID/04029/Institute for Sustainability and Innovation in Structural Engineering (ISISE), and under the Associate Laboratory Advanced Production and Intelligent Systems ARISE under reference LA/P/0112/2020.

6. REFERENCES

[1] W. H. Organization, *Compendium of WHO and other UN guidance on health and environment: version with International Classification of Health Intervention (ICHI) codes*: World Health Organization, 2024.

[2] J. P. Arenas and M. J. Crocker, "Recent trends in porous sound-absorbing materials," *Sound & vibration*, vol. 44, pp. 12-18, 2010.

[3] S. Nakanishi, "Broadband sound absorption by acoustic metasurface of planar array of small Helmholtz resonators," *Acoustical Science and Technology*, vol. advpub, 2024.

[4] N. Jiménez, O. Umnova, and J.-P. Groby, "Acoustic waves in periodic structures, metamaterials, and porous media," *Ch. the Transfer Matrix Method in Acoustics, Springer International Publishing, Cham*, pp. 103-164, 2021.

[5] H. Liu and F. Wang, "A novel semi-analytical meshless method for the thickness optimization of porous material distributed on sound barriers," *Applied Mathematics Letters*, vol. 147, p. 108844, 2024.

[6] J.-P. Groby, O. Dazel, A. Duclos, L. Boeckx, and L. Kelders, "Enhancing the absorption

coefficient of a backed rigid frame porous layer by embedding circular periodic inclusions," *The Journal of the Acoustical Society of America*, vol. 130, pp. 3771-3780, 2011.

[7] J.-P. Groby, C. Lagarrigue, B. Brouard, O. Dazel, V. Tournat, and B. Nennig, "Enhancing the absorption properties of acoustic porous plates by periodically embedding Helmholtz resonators," *The Journal of the Acoustical Society of America*, vol. 137, pp. 273-280, 2015.

[8] J. Allard and N. Atalla, *Propagation of sound in porous media: modelling sound absorbing materials, John Wiley & Sons, Chichester (United Kingdom), 2nd Edition, 2009*.

[9] A. D. Pierce, *Acoustics: an introduction to its physical principles and applications*: Springer, 2019.

[10] K. V. Horoshenkov and M. J. Swift, "The acoustic properties of granular materials with pore size distribution close to log-normal, *The Journal of the Acoustical Society of America*, Vol 110 (5), 2001, pp 2371-2378."

[11] M. R. Stinson, "The propagation of plane sound waves in narrow and wide circular tubes, and generalization to uniform tubes of arbitrary cross‐sectional shape," *The Journal of the Acoustical Society of America*, vol. 89, pp. 550-558, 1991.

[12] K.-J. Bathe, *Finite element procedures, Prentice-Hall, Englewood Cliffs, New Jersey (United States of America), 2nd Edition, 2014*.

[13] ISO, "ISO 10534-2: *Acoustics — Determination of sound absorption coefficient and impedance in impedance tubes - Part 2: Transfer-function method*, Genève, 1998," ed.

[14] M. Pereira, J. Carbajo San Martín, L. Godinho, P. Amado-Mendes, D. Mateus, and J. Ramis-Soriano, "Acoustic behavior of porous concrete. Characterization by experimental and inversion methods, Materiales de Construcción, Vol 69 (336), 2019, pp e202."

[15] L. Lourenço de Sousa, L. Pereira, L. Godinho, and P. A. Mendes, "Acoustic properties of porous concrete-Experiments and modelling, *INTER-NOISE and NOISE-CON Congress and Conference Proceedings 2020*, Seul, Korea, August 23-26, 2020, Vol 261 No 6, pp 127-137, Institute of Noise Control Engineering."

[16] L. Lourenço de Sousa, L. Pereira, D. Ramos, L. Godinho, and P. A. Mendes, "Acoustic absorption of porous concrete – normal incidence vs diffuse field conditions, *Euronoise Congress and Conference Proceedings 2021*, Madeira, Portugal, October 25-27, 2021, pp 239-248."

[17] L. Sousa, L. Pereira, D. Montes-González, D. Ramos, P. Amado-Mendes, J. M. Barrigón-Morillas, *et al.*, "Experimental Analysis and Simulation of a Porous Absorbing Layer for Noise Barriers," *Applied Sciences*, vol. 13, p. 2638, 2023.

[18] Y. Miki, "Acoustical properties of porous materials-Modifications of Delany-Bazley models, *Journal of the Acoustical Society of Japan*, Vol 11 (1), 1990, pp 19-24."